Tensor-Network Codes

Terry Farrelly,[1,*] Robert J. Harris,[1] Nathan A. McMahon,[1,2] and Thomas M. Stace[1]
[1]ARC Centre for Engineered Quantum Systems, School of Mathematics and Physics, The University of Queensland, St. Lucia, Queensland 4072, Australia
[2]Department of Physics, Friedrich-Alexander University Erlangen-Nürnberg (FAU), D-91058 Erlangen, Germany

(Received 21 September 2020; accepted 23 June 2021; published 23 July 2021)

We introduce tensor-network stabilizer codes which come with a natural tensor-network decoder. These codes can correspond to any geometry, but, as a special case, we generalize holographic codes beyond those constructed from perfect or block-perfect isometries, and we give an example that corresponds to neither. Using the tensor-network decoder, we find a threshold of 18.8% for this code under depolarizing noise. We show that, for holographic codes, the exact tensor-network decoder (with no bond-dimension truncation) has polynomial complexity in the number of physical qubits, even for locally correlated noise, making this the first efficient decoder for holographic codes against Pauli noise and, also, a rare example of a decoder that is both efficient and exact.

DOI: 10.1103/PhysRevLett.127.040507

Tensor networks are a powerful tool in several branches of physics [1], so it is not surprising that they are also useful in quantum error correction. An early example of this was the use of matrix-product states to approximate the maximum likelihood decoder (the optimal decoder) for the surface code [2]. This algorithm (with modifications) was applied to biased noise [3,4] and correlated noise [5] on the surface code. Another approach using tensor networks to decode the surface code involved representing code states by projected entangled pair states and then finding the effective channel due to noise on the logical degrees of freedom [6,7]. This allowed one to go beyond Pauli noise and consider less-studied but important error models. A general method for decoding using tensor networks involved representing the encoding unitaries by a tensor network [8,9].

Tensor networks also arose in holographic error correcting codes, which are toy models of the AdS/CFT correspondence [10–18]. The idea is that the bulk degrees of freedom of a system in two-dimensional hyperbolic space (logical qubits) are encoded in the boundary degrees of freedom (physical qubits). This is analogous to AdS/CFT, where a strongly coupled gravity theory in the bulk is equivalent to a conformal field theory on the boundary [19]. Holographic error correcting codes can reproduce much of the entanglement structure expected in AdS/CFT [10], e.g., the Ryu-Takayanagi formula [20].

The holographic codes of [10] were constructed from a strongly constrained isometry called a perfect tensor. Afterwards, this class of tensors was replaced by the larger class of block perfect tensors (or equivalently perfect tangles) [21,22], leading to the construction of Calderbank-Shor-Steane (CSS) holographic codes [21]. One example was constructed from the seven-qubit Steane code [23], which was decoded with an integer optimization algorithm [24] for Pauli noise (though the decoder is not efficient).

In this Letter, we introduce tensor-network stabilizer codes, which allow us to construct larger stabilizer codes out of smaller ones. These codes naturally come with a tensor-network decoder (which is different but can be related to the tensor-network decoder of [8]), which calculates the relevant probabilities for the maximum likelihood decoder. Special cases of tensor-network codes include concatenated and holographic codes. Here, we use tensor-network codes to generalize holographic codes beyond perfect or block-perfect isometries. We give an example corresponding to neither perfect nor block perfect isometries and which we decode using the tensor-network decoder to find a threshold of 18.8% under depolarizing noise. This compares quite well to the threshold for the surface code of 18.9% [25]. Our key outcome is that the exact tensor-network decoder is computationally efficient for holographic codes, with a polynomial runtime in the number of physical qubits, making it the first efficient (and exact) decoder for holographic codes against uncorrelated (or even weakly correlated) Pauli noise.

Stabilizer codes.—In stabilizer codes [26–29], logical operators and stabilizers are elements of the n-qubit Pauli group $\mathcal{G}_n$, which consists of all operators like $z\sigma^{i_1} \otimes \cdots \otimes \sigma^{i_n}$, where $z \in \{\pm 1, \pm i\}$. Here, $\sigma^0 = \mathbb{1}$, $\sigma^1 = X$, $\sigma^2 = Y$, and $\sigma^3 = Z$, which are the single-qubit identity operator and three Pauli operators, respectively.

We consider Pauli noise on the physical qubits, so errors are elements of $\mathcal{G}_n$. For the example holographic code, we

will consider depolarizing noise on the physical qubits, where each physical qubit is subject to the quantum channel

$$D(\rho) = (1-p)\rho + \frac{p}{3}\sum_{i=1}^{3}\sigma^i\rho\sigma^i, \tag{1}$$

where $0 \le p \le 1$ is the probability of an error affecting the qubit.

The subspace encoding logical information, the code space, is fixed by an Abelian group of operators $\mathcal{S} \subset \mathcal{G}_n$ called stabilizers. For any state $|\psi\rangle$ in the code space, $S|\psi\rangle = |\psi\rangle$ for every $S \in \mathcal{S}$. If $\mathcal{S}$ has r independent generators S_i, the code space has dimension 2^{n-r} corresponding to $k = n - r$ logical qubits [28].

Logical operators on the encoded qubits form a non-Abelian group $\mathcal{L} \subset \mathcal{G}_n$. This group is generated by the k X-type and k Z-type operators, which we may call X_α and Z_α, where $\alpha \in \{1, \ldots, k\}$. These commute with the stabilizers and satisfy $X_\alpha Z_\beta = (-1)^{\delta_{\alpha\beta}} Z_\alpha X_\beta$.

The final important (Abelian) group of operators are pure errors $\mathcal{E} \subset \mathcal{G}_n$. This group is generated by the $n-k$ operators E_i which are chosen to satisfy $E_i S_j = (-1)^{\delta_{ij}} S_j E_i$ with $E_i^2 = \mathbb{1}$. That such generators exist is shown in Sec. A of [30]. The full Pauli group is generated by all E_i, S_i, X_α, and Z_α.

To detect errors, we measure the stabilizer generators S_i giving eigenvalues $s_i = \pm 1$. The syndrome $\vec{s}$ is the collection of these measurement outcomes. We denote the pure error corresponding to syndrome $\vec{s}$ by $E(\vec{s})$, meaning $E(\vec{s})$ is the product of all E_i such that $s_i = -1$. $E(\vec{s})$ is not the only error with syndrome $\vec{s}$. Any error $E' = LSE(\vec{s})$, for any $L \in \mathcal{L}$ and any $S \in \mathcal{S}$, will have the same syndrome. Deciding which operation to apply to correct whichever (if any) error has occurred is called decoding, a difficult problem in general [32,33].

Tensor-network error correcting codes.—Let us introduce tensors describing arbitrary stabilizer codes. We represent operators by strings of integers, e.g., the stabilizer $XZYYX\mathbb{1} = \sigma^1\sigma^3\sigma^2\sigma^2\sigma^1\sigma^0$ is represented by the string (1,3,2,2,1,0). Then, for each logical operator $L \in \mathcal{L}$, we define the rank-n tensor (which is the indicator function for all operators in the class L)

$$T(L)_{(g_1,\ldots,g_n)} = \begin{cases} 1 & \text{if } \sigma^{g_1} \otimes \cdots \otimes \sigma^{g_n} \in \mathcal{S}L \\ 0 & \text{otherwise} \end{cases}, \tag{2}$$

where $g_j \in \{0,1,2,3\}$ and $\mathcal{S}L$ is the set of all operators of the form SL with $S \in \mathcal{S}$. In other words, $\mathcal{S}L$ is the coset of $\mathcal{S}$ with respect to the logical operator L. For example, $T(\mathbb{1})_{(g_1,\ldots,g_n)}$ is nonzero only when $\sigma^{g_1} \otimes \cdots \otimes \sigma^{g_n}$ is a stabilizer, so $T(\mathbb{1})$ describes the stabilizer group (except for the signs of the stabilizers, but once these are fixed for the generators, they are determined for the whole group).

TABLE I. Stabilizer generators and logical operators for the $[\![6,1,3]\!]$ code from [34]. Their action on physical qubits is shown in columns 1–6, and their action on the logical code space is shown in column 0. We can also view these seven operators as stabilizing a state on seven qubits 0–6.

Qubit	0	1	2	3	4	5	6
S_1	$\mathbb{1}$	Z	$\mathbb{1}$	Z	$\mathbb{1}$	$\mathbb{1}$	$\mathbb{1}$
S_2	$\mathbb{1}$	X	Z	Y	Y	X	$\mathbb{1}$
S_3	$\mathbb{1}$	X	X	X	X	Z	$\mathbb{1}$
S_4	$\mathbb{1}$	$\mathbb{1}$	Z	Z	X	$\mathbb{1}$	X
S_5	$\mathbb{1}$	X	Y	X	Y	$\mathbb{1}$	Z
X_1	X	X	Z	X	Z	$\mathbb{1}$	$\mathbb{1}$
Z_1	Z	X	Y	Y	X	$\mathbb{1}$	$\mathbb{1}$

Similarly, for a code with a single logical qubit, $T(X)_{(g_1,\ldots,g_n)}$ describes the class of the logical X operator.

These tensors are not isometries, rather they describe the code in a simple way. The tensors are agnostic about encoding unitaries, but they can be related to encoding unitaries and the tensors of [8] (see [30]).

For example, take the six-qubit code of [34], which encodes one logical qubit into six physical qubits with stabilizer generators and logical operators summarized in Table I. The tensors for this code $T^1(L)_{(g_1,\ldots,g_6)}$ have 32 nonzero values for each possible $L \in \{\mathbb{1}, X, Y, Z\}$, e.g., $T^1(X)_{(131300)} = 1$. We can define another code with no logical qubits (i.e., a stabilizer state) on seven physical qubits by taking the six-qubit code plus an extra qubit 0 with all operators in Table I as stabilizers. Let us denote this code tensor by $T^0_{(g_0,\ldots,g_6)}$, so, e.g., $T^0_{(3122100)} = 1$.

The benefit of describing codes by these code tensors is that we can combine several tensors together by contracting tensor legs to get new stabilizer codes, which come with a natural tensor-network decoder. If the tensor network can be efficiently contracted, the code can also be efficiently decoded. We will see an example of this for holographic codes, where the decoder is efficient without any approximations. The following theorem explains how to join code tensors to get new stabilizer codes (see, also, Fig. 1).

Theorem 1.—Consider two code tensors $T(L)_{(g_1,\ldots,g_n)}$ and $T'(L')_{(h_1,\ldots,h_{n'})}$ which have n and n' physical qubits and k and k' logical qubits, respectively. We get new tensors describing a new stabilizer code by contracting indices (for simplicity, choose qubits 1 to l for both codes), i.e.,

$$T_{\text{new}}(L \otimes L')_{(g_{l+1},\ldots,g_n,h_{l+1},\ldots,h_{n'})} = \sum_{j_1,\ldots,j_l \in \{0,1,2,3\}} T(L)_{(j_1,\ldots,j_l,g_{l+1},\ldots,g_n)} T'(L')_{(j_1,\ldots,j_l,h_{l+1},\ldots,h_{n'})},$$

provided either one of these codes can distinguish any Pauli error on qubits 1 to l. T_{new} describes a stabilizer code with $n + n' - 2l$ physical qubits and $k + k'$ logical qubits. (Proved in [30].)

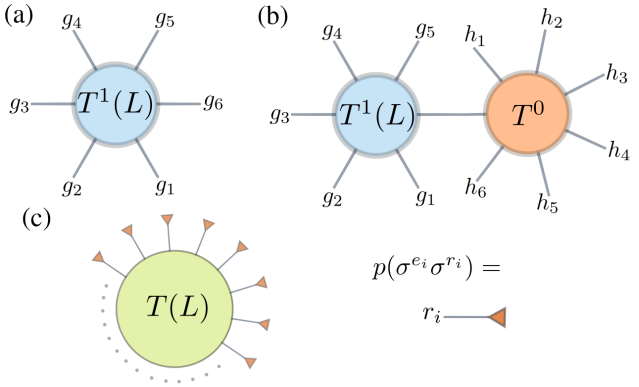

FIG. 1. Tensor-network codes: (a) the tensor $T^1(L)_{(g_1,\ldots,g_6)}$ describing a six-qubit code, where L denotes logical operators. (b) Applying Theorem 1 to build a new code tensor by contracting the sixth index of $T^1(L)_{(g_1,\ldots,g_6)}$ with the first index of $T^0_{(h_0,\ldots,h_6)}$ to get a $[\![11,1,3]\!]$ code. (c) A tensor-network decoder calculates a probability for each logical operator L (the correction operator is determined by finding the maximum of these probabilities) by contracting the code tensor with rank-one tensors $p(\sigma^{e_i}\sigma^{r_i})$ for each physical qubit i, with index r_i (e_i is fixed by the syndrome and, so, is not summed over). This is an implementation of maximum-likelihood decoding.

This means we can build larger codes using small tensors as building blocks. The tensor network can have any geometry and the component tensors can have any number of logical qubits. It is simple to check if a tensor can be contracted onto another tensor to get a new stabilizer code: we just check if one of them can distinguish all different Pauli errors on the qubits corresponding to the contracted legs, which is equivalent to there existing an isometry from those legs (plus logical qubits) to the rest [30]. Theorem 1 allows us to iteratively build up very large codes with consistency guaranteed, and, as we will see, it is exactly these tensors $T(L)$ that are contracted in the tensor-network decoder. Also, it is straightforward to find stabilizer generators and pure errors [30].

For example, we can contract index g_6 of $T^1(L)_{(g_1,\ldots,g_6)}$ and index h_0 of $T^0_{(h_0,\ldots,h_6)}$ as shown in Fig. 1. The six-qubit code can distinguish any single-qubit error on its sixth qubit (see Table I), meaning the resulting tensor describes a stabilizer code with 11 physical qubits and one logical qubit.

Other examples are concatenated codes (or generalized concatenated codes [35,36]), e.g., for the six-qubit code

$$\begin{aligned} &T^{\mathrm{conc}}(L)_{(h_1,\ldots,h_{36})} \\ &\quad = T^1(L)_{(g_1,\ldots,g_6)} T^0_{(g_1,h_1,\ldots,h_6)} T^0_{(g_2,h_7,\ldots,h_{12})} \\ &\qquad \times T^0_{(g_3,h_{13},\ldots,h_{18})} T^0_{(g_4,h_{19},\ldots,h_{24})} T^0_{(g_5,h_{25},\ldots,h_{30})} T^0_{(g_6,h_{31},\ldots,h_{36})}, \end{aligned}$$

where repeated indices are contracted. An interesting example of tensor-network codes will be holographic codes.

Finally, these tensor-network codes should not be confused with quantum tensor product codes [37], where one constructs codes via tensor products of parity-check matrices.

Maximum likelihood decoding via tensor networks.— The optimal decoder for quantum error correction is the maximum likelihood decoder, which finds the error correction operator that is most likely to return the system to the correct code state, given the syndrome.

Any error corresponding to syndrome $\vec{s}$ has the form $E(\vec{s})SL$ for some $L \in \mathcal{L}$ and $S \in \mathcal{S}$. Because $E(\vec{s})SL$ has the same effect on the code space for any S, we need to calculate

$$\chi(L,\vec{s}) = \sum_{S\in\mathcal{S}} \mathrm{prob}[E(\vec{s})SL] \tag{3}$$

for each $L \in \mathcal{L}$, where $\mathrm{prob}[E(\vec{s})SL]$ is the probability that the error $E(\vec{s})SL$ occurred on the physical qubits. Then the correction operator we should apply is $\bar{L}E(\vec{s})$, where $\bar{L} = \mathrm{argmax}_L \chi(L,\vec{s})$.

Calculating $\chi(L,\vec{s})$ for many physical qubits is difficult in general [33]. Luckily, sometimes it is possible to write $\chi(L,\vec{s})$ as a tensor network that can be contracted efficiently. This idea was introduced for the surface code in [2] and for other codes via a circuit description in [8]. Writing an error as $E(\vec{s})SL = \sigma^{a_1} \otimes \cdots \otimes \sigma^{a_n}$ with $a_i \in \{0,1,2,3\}$, then, for the case of independent noise on each qubit, $\mathrm{prob}(\sigma^{a_1} \otimes \cdots \otimes \sigma^{a_n}) = p_1(\sigma^{a_1}) \times \cdots \times p_n(\sigma^{a_n})$, where $p_i(\sigma^{a_i})$ is the probability that σ^{a_i} will act on qubit i due to the noise. For independent and identically distributed depolarizing noise, which we have already defined in Eq. (1), $p(\sigma^{a_i}) = (1-p)\delta_{0a_i} + p/3(1-\delta_{0a_i})$. If we write $E(\vec{s}) = \sigma^{e_1} \otimes \cdots \otimes \sigma^{e_n}$, then we have

$$\chi(L,\vec{s}) = \sum_{r_1,\ldots,r_n\in\{0,1,2,3\}} T(L)_{(r_1,\ldots,r_n)} \prod_{i=1}^{n} p_i(\sigma^{e_i}\sigma^{r_i}), \tag{4}$$

where $T(L)_{(r_1,\ldots,r_n)}$ is the code tensor defined in Eq. (2). This tensor network contraction is sketched in Fig. 1. We should think of $p(\sigma^{e_i}\sigma^{r_i})$ as a one-leg tensor associated to physical qubit i, with index r_i, as in Fig. 1. Index e_i is fixed because the pure error $E(\vec{s})$ is fixed by the syndrome. For correlated noise $\prod_{i=1}^n p_i(\cdot)$ will be replaced by $\mathrm{prob}(\cdot)$, though for the tensor network to be efficiently contractible, restrictions on $\mathrm{prob}(\cdot)$ would be necessary, like finite correlation length, e.g., factored noise [5].

For large codes, $T(L)_{(r_1,\ldots,r_n)}$ can be extremely complex and contraction quickly becomes difficult with increasing n. In [2], for the surface code, the strategy was to decompose the tensor $T(L)$ (which described a code with only one logical qubit) into smaller tensors. In [5], maximum likelihood decoding was recast as a calculation of partition functions via tensor networks, which is also

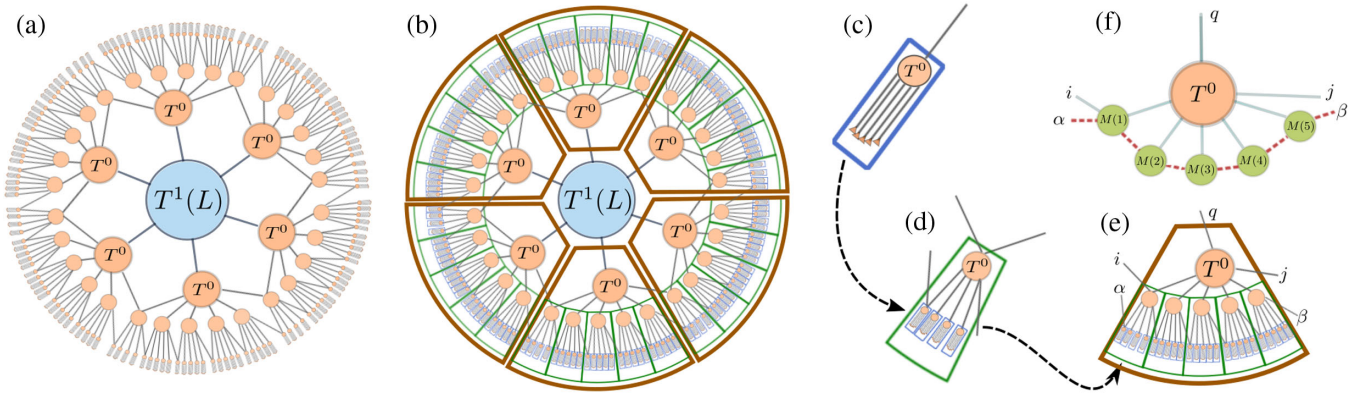

FIG. 2. (a) Tensor network for a radius-four holographic code. The central tensor $T^1(L)$ (with one logical qubit) has six legs, whereas all other tensors T^0 with no logical qubits have seven legs. (b) Contraction order: starting from the outside, contract inwards. After the first contractions (c), we have tensors at radius four, which are enclosed inside the blue boxes. After the next contraction (d), we have tensors at radius three, enclosed in green boxes. After another round of contractions (e), we have the tensor enclosed in the brown box. Finally, these tensors are contracted with the central tensor, colored blue in (b). (f) Generic form of a tensor contraction: $M(k)$ are the results of previous contractions, with bond legs marked by dashed lines.

applied to the surface code. In [8], the encoding unitary circuit was represented by tensors, but the method can be related to Eq. (4) [30]. Our approach is to build tensor-network codes out of many smaller code tensors (with any number of logical qubits) with the goal that contraction be efficient. Now, we will consider an example for holographic codes.

Holographic codes as tensor-network codes.—Using tensor-network codes, we can generalize previous incarnations of holographic codes, which relied on perfect [10] or block-perfect tensors or perfect tangles [21,22]. Let us use the six-qubit code as a building block, which is neither perfect nor block perfect (for any ordering of the indices).

We start with a central six-qubit code tensor $T^1(L)$ as in Fig. 2. Then, we contract with the six tensors T^0 at radius two, each of which has one ingoing leg contracted with an outgoing leg of the central tensor, getting a radius-two code. To get a radius-three code, we contract T^0 tensors with each outgoing leg of the radius-two tensors, but now, some radius-three tensors have two legs contracted with two neighboring radius-two tensors, as shown in Fig. 2. This pattern repeats until we reach the code radius R, where any external legs correspond to physical qubits. From Theorem 1, we know that this is a valid stabilizer code, because T^0 can distinguish two-qubit errors on the qubits corresponding to the ingoing legs. (We choose the index ordering so that each tensor $T^0_{(g_0,\ldots,g_6)}$ at radius $r+1$ has either index g_6 contracted with one tensor at radius r or indices g_5 and g_6 contracted with two tensors at radius r.)

To decode, we contract the tensor network to calculate $\chi(L,\vec{s})$ for each $L \in \{\mathbb{1}, X, Y, Z\}$. As shown in Fig. 2, we contract from the outside of the network in. The bond dimension $D[r]$ of the tensors at radius r obeys $D[r] = 4^{R-r}$ as we contract inwards. Even without bond-dimension truncation, this contraction method is efficient, meaning the number of operations is polynomial in the number of physical qubits n. The total number of operations N satisfies [30]

$$N = bn^{\max(n_{\mathrm{mat}}/c,1)}, \tag{5}$$

where c and b are constants, and we have assumed the complexity of multiplying two $N \times N$ matrices is $O(N^{n_{\mathrm{mat}}})$, so $n_{\mathrm{mat}} \simeq 2.37$ in the best case [38]. For holographic codes with tensors having more than seven legs (as in this case), $c \geq 1$. Otherwise, $0 < c \leq 1$. This should be contrasted with the method of [2] for the surface code, which is also polynomial in the number of physical qubits, but relies on bond-dimension truncation as an approximation.

We applied this contraction algorithm to our example holographic code in the presence of depolarizing noise. Monte Carlo simulation results are shown in Fig. 3. We see a threshold for the code at 18.8% [30], which compares well with the threshold for the surface code of 18.9% [25]. The rate of this code in terms of distance d is estimated to be $1/n \propto 1/d^{1.64}$ [30], which scales slightly better than the surface code ($\propto 1/d^2$).

Conclusions.—We described stabilizer codes by tensors and showed that we can combine codes by contracting tensor legs to get larger stabilizer codes. These tensor-network stabilizer codes come with a natural tensor-network decoder. We applied this to holographic codes generalizing previous constructions and found a new code with a threshold of 18.8% under depolarizing noise. We showed that the computational complexity of decoding holographic codes via the maximum likelihood decoder is polynomial in the number of physical qubits even in the exact case, with no bond-dimension truncation. Thus, the decoder is a rare example of an exact and efficient decoder.

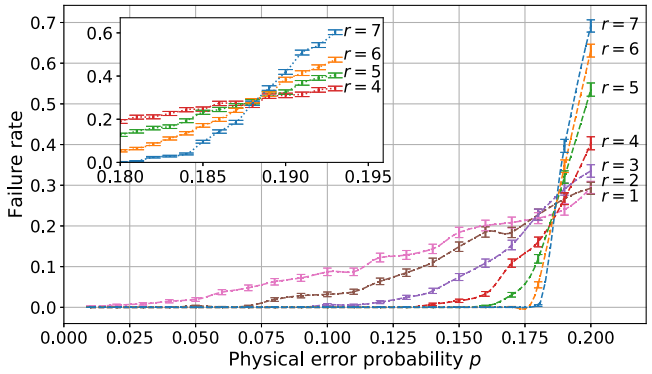

FIG. 3. Failure rates for the (asymptotically zero-rate) six-qubit holographic code versus the single-qubit error probability p for different code radii. Lines are to guide the eye between failure rates within a fixed code size. Inset: expanded view of failure rates close to the threshold of 18.8% [30].

(Other examples are concatenated [39] and convolutional codes [40].) Furthermore, even for a single contraction of the tensor network, many operations can be done in parallel, greatly speeding up decoding. These results are a key step toward using holographic codes in practice, especially for CSS holographic codes [21], which have a cluster state construction [41], making them suitable for photonic systems. Finally, the efficiency of our contraction scheme suggests the method may be useful for calculating, e.g., partition functions of locally interacting systems on hyperbolic tilings.

The authors would like to thank Aidan Strathearn for useful discussions. This work was supported by the Australian Research Council Centres of Excellence for Engineered Quantum Systems (EQUS, Grant No. CE170100009) and the Asian Office of Aerospace Research and Development (AOARD) Grant No. FA2386-18-14027. Numerical simulations were performed on The University of Queensland's School of Mathematics and Physics Core Computing Facility "getafix" (with thanks to Dr. L. Elliott and I. Mortimer for computing support).

*farreltc@tcd.ie

[1] J. C. Bridgeman and C. T. Chubb, Hand-waving and interpretive dance: An introductory course on tensor networks, J. Phys. A **50**, 223001 (2017).
[2] S. Bravyi, M. Suchara, and A. Vargo, Efficient algorithms for maximum likelihood decoding in the surface code, Phys. Rev. A **90**, 032326 (2014).
[3] D. K. Tuckett, A. S. Darmawan, C. T. Chubb, S. Bravyi, S. D. Bartlett, and S. T. Flammia, Tailoring Surface Codes for Highly Biased Noise, Phys. Rev. X **9**, 041031 (2019).
[4] D. K. Tuckett, S. D. Bartlett, and S. T. Flammia, Ultrahigh Error Threshold for Surface Codes with Biased Noise, Phys. Rev. Lett. **120**, 050505 (2018).
[5] C. T. Chubb and S. T. Flammia, Statistical mechanical models for quantum codes with correlated noise, Ann. Inst. Henri Poincaré Comb. Phys. Interact. **8**, 269 (2021).
[6] A. S. Darmawan and D. Poulin, Tensor-Network Simulations of the Surface Code under Realistic Noise, Phys. Rev. Lett. **119**, 040502 (2017).
[7] A. S. Darmawan and D. Poulin, Linear-time general decoding algorithm for the surface code, Phys. Rev. E **97**, 051302 (R) (2018).
[8] A. J. Ferris and D. Poulin, Tensor Networks and Quantum Error Correction, Phys. Rev. Lett. **113**, 030501 (2014).
[9] A. J. Ferris and D. Poulin, Branching MERA codes: A natural extension of classical and quantum polar codes, in *2014 IEEE International Symposium on Information Theory* (2014), pp. 1081–1085.
[10] F. Pastawski, B. Yoshida, D. Harlow, and J. Preskill, Holographic quantum error-correcting codes: Toy models for the bulk/boundary correspondence, J. High Energy Phys. 06 (2015) 149.
[11] J. I. Latorre and G. Sierra, Holographic codes, arXiv: 1502.06618.
[12] P. Hayden, S. Nezami, X.-L. Qi, N. Thomas, M. Walter, and Z. Yang, Holographic duality from random tensor networks, J. High Energy Phys. 11 (2016) 9.
[13] G. Evenbly, Hyperinvariant Tensor Networks, and Holography, Phys. Rev. Lett. **119**, 141602 (2017).
[14] A. Jahn, M. Gluza, F. Pastawski, and J. Eisert, Holography and criticality in match gate tensor networks, Sci. Adv. **5**, eaaw0092 (2019).
[15] A. Jahn, M. Gluza, F. Pastawski, and J. Eisert, Majorana dimers and holographic quantum error-correcting codes, Phys. Rev. Research **1**, 033079 (2019).
[16] T. Kohler and T. Cubitt, Toy models of holographic duality between local Hamiltonians, J. High Energy Phys. 08 (2019) 17.
[17] T. J. Osborne and D. E. Stiegemann, Dynamics for holographic codes, J. High Energy Phys. 04 (2020) 154.
[18] P. Mazurek, M. Farkas, A. Grudka, M. Horodecki, and M. Studziński, Quantum error-correction codes and absolutely maximally entangled states, Phys. Rev. A **101**, 042305 (2020).
[19] D. Harlow, Jerusalem lectures on black holes and quantum information, Rev. Mod. Phys. **88**, 015002 (2016).
[20] S. Ryu and T. Takayanagi, Holographic Derivation of Entanglement Entropy from the anti–de Sitter Space/Conformal Field Theory Correspondence, Phys. Rev. Lett. **96**, 181602 (2006).
[21] R. J. Harris, N. A. McMahon, G. K. Brennen, and T. M. Stace, Calderbank-Shor-Steane holographic quantum error-correcting codes, Phys. Rev. A **98**, 052301 (2018).
[22] J. Berger and T. J. Osborne, Perfect tangles, arXiv: 1804.03199.
[23] A. Steane, Multiple-particle interference and quantum error correction, Proc. R. Soc. Ser. A **452**, 2551 (1996).
[24] R. J. Harris, E. Coupe, N. A. McMahon, G. K. Brennen, and T. M. Stace, Decoding holographic codes with an integer optimization decoder, Phys. Rev. A **102**, 062417 (2020).
[25] H. Bombin, R. S. Andrist, M. Ohzeki, H. G. Katzgraber, and M. A. Martin-Delgado, Strong Resilience of Topological

Codes to Depolarization, Phys. Rev. X **2**, 021004 (2012).
[26] D. Gottesman, Stabilizer codes and quantum error correction, Ph.D. thesis, California Institute of Technology, 1997.
[27] D. Gottesman, An introduction to quantum error correction and fault-tolerant quantum computation, arXiv:0904.2557.
[28] M. A. Nielsen and I. L. Chuang, *Quantum Computation and Quantum Information* (Cambridge University Press, Cambridge, England, 2010).
[29] J. Roffe, Quantum error correction: An introductory guide, Contemp. Phys. **60**, 226 (2019).
[30] See Supplemental Material at http://link.aps.org/supplemental/10.1103/PhysRevLett.127.040507 which includes Ref. [31].
[31] C. Wang, J. Harrington, and J. Preskill, Confinement-Higgs transition in a disordered gauge theory and the accuracy threshold for quantum memory, Ann. Phys. (Amsterdam) **303**, 31 (2003).
[32] M.-H. Hsieh and F. Le Gall, NP-hardness of decoding quantum error-correction codes, Phys. Rev. A **83**, 052331 (2011).
[33] P. Iyer and D. Poulin, Hardness of decoding quantum stabilizer codes, IEEE Trans. Inf. Theory **61**, 5209 (2015).
[34] B. Shaw, M. M. Wilde, O. Oreshkov, I. Kremsky, and D. A. Lidar, Encoding one logical qubit into six physical qubits, Phys. Rev. A **78**, 012337 (2008).
[35] M. Grassl, P. Shor, G. Smith, J. Smolin, and B. Zeng, Generalized concatenated quantum codes, Phys. Rev. A **79**, 050306(R) (2009).
[36] Y. Wang, B. Zeng, M. Grassl, and B. C. Sanders, Stabilizer formalism for generalized concatenated quantum codes, in *2013 IEEE International Symposium on Information Theory* (2013), pp. 529–533.
[37] J. Fan, Y. Li, M.-H. Hsieh, and H. Chen, On quantum tensor product codes, Quantum Inf. Comput. **17**, 1105 (2017).
[38] F. Le Gall, Powers of tensors and fast matrix multiplication, in *Proceedings of the 39th International Symposium on Symbolic and Algebraic Computation* (2014), pp. 296–303.
[39] D. Poulin, Optimal and efficient decoding of concatenated quantum block codes, Phys. Rev. A **74**, 052333 (2006).
[40] E. Pelchat and D. Poulin, Degenerate Viterbi decoding., IEEE Trans. Inf. Theory **59**, 3915 (2013).
[41] A. Bolt, G. Duclos-Cianci, D. Poulin, and T. M. Stace, Foliated Quantum Error-Correcting Codes, Phys. Rev. Lett. **117**, 070501 (2016).